Journal of Applied Physics

High-order harmonics generation under quasi-phase matched conditions in silver, boron, and silver sulfide plasmas of different configurations

Cite as: J. Appl. Phys. **125**, 153101 (2019); https://doi.org/10.1063/1.5089223
Submitted: 17 January 2019 . Accepted: 02 April 2019 . Published Online: 19 April 2019

Rashid A. Ganeev, Ganjaboy S. Boltaev, Vyacheslav V. Kim, Pavel V. Redkin, and Chunlei Guo

Journal of Applied Physics ARTICLE scitation.org/journal/jap

High-order harmonics generation under quasi-phase matched conditions in silver, boron, and silver sulfide plasmas of different configurations

Cite as: J. Appl. Phys. **125**, 153101 (2019); doi: 10.1063/1.5089223
Submitted: 17 January 2019 · Accepted: 2 April 2019 ·
Published Online: 19 April 2019

Rashid A. Ganeev,[1,2,a)] Ganjaboy S. Boltaev,[1] Vyacheslav V. Kim,[1] Pavel V. Redkin,[1] and Chunlei Guo[1,3,b)]

AFFILIATIONS

[1]The Guo China-US Photonics Laboratory, State Key Laboratory of Applied Optics, Changchun Institute of Optics, Fine Mechanics and Physics, Chinese Academy of Sciences, Changchun 130033, China
[2]Faculty of Physics, Voronezh State University, 1 University Square, Voronezh 394018, Russia
[3]The Institute of Optics, University of Rochester, Rochester, New York 14627, USA

[a)]rashid_ganeev@mail.ru
[b)]guo@optics.rochester.edu

ABSTRACT

The application of advanced methods for high-order harmonics enhancement allows the formation of conditions for phase matching of the generated harmonics in different ranges of extreme ultraviolet. We demonstrate quasi-phase matching (QPM) of the high-order harmonics generated in the plasmas containing silver microparticles and atoms, and silver sulfide molecules. The groups of harmonics in the range of 30th to 40th orders at QPM conditions prevail over the lower orders of harmonics. In most cases, the lower-order harmonics disappeared from the generated spectra at QPM conditions. The 22× enhancement factor of QPM harmonics and the 3×10^{-5} conversion efficiency for a maximally enhanced harmonic were demonstrated in the case of silver microparticle-contained plasma in the 47–67 eV energy range.

I. INTRODUCTION

Currently, high-order harmonics generation (HHG) of femtosecond laser pulses is considered the most reliable method allowing the formation of coherent radiation sources in the extreme ultraviolet (XUV) spectral range. Such short-wavelength sources are useful for the fundamental and applied studies in various fields of physical, chemical, and life sciences. However, so far, only low conversion efficiencies of HHG ($\sim 10^{-5}$) have been obtained, despite the numerous attempts to increase the harmonic yield using various methods.[1]

Higher conversion efficiency and, thus, an increase in the photon flux of the harmonics radiation is a requirement for practical applications of coherent XUV sources. A largely unexplored approach for this purpose is the harmonic generation in plasmas, which provides various options in the nonlinear spectroscopy of materials compared with the well-developed technique of harmonics generation in gases. Two-color pump (TCP)- and three-color pumps of plasma, nanoparticle (NP)-induced growth of a whole ensemble of harmonics, resonance enhancement of single harmonic, and nonlinear medium's length extension have been applied to amend this process in laser-produced plasmas (LPP).

Previous studies have shown that enhanced harmonics can be produced at quasi-phase matching (QPM) conditions after one uses the multijet LPP by inserting a multislit mask (MSM) in front of the ablated surface instead of the extended imperforated plasma formations,[2,3] similar to the earlier reported achievements in the case of the multijet gas targets.[4–7] Notice that the formation of QPM conditions in the laser plasmas is a more complicated task compared with the gas media due to general problems related to precise control of concentration of ions and electrons in the interaction area.

Recently, a dependence of QPM-induced enhancement on the distance between plasma jets was analyzed using ablation of rotating disks.[3] The importance of fine tuning and control of the quasi-phase matching for high-order harmonics generation (QPM-HHG) has motivated us to investigate the influence of the spacing between

plasma jets on this process at different conditions of multijet plasma (MJP) formation. Additionally, a search for new plasma media suitable for QPM-HHG, such as nanoparticles and microparticles (MPs) and molecules, broadens the applications of this concept and allows determining better conditions for HHG. Notice that most previous QPM studies were performed in the plasmas produced during ablation of bulk silver, though other metal plasmas were also probed for these purposes.

In this paper, we demonstrate, for the first time, QPM-HHG in the plasmas containing silver microparticles and atoms, and silver sulfide molecules. We present different combinations of MJP formations to determine the best choice for the generation of the groups of enhanced harmonics in the 20–60 nm spectral range.

II. EXPERIMENTAL ARRANGEMENTS

In these QPM-HHG studies, 30 fs, 800 nm, 1 kHz and 200 ps, 800 nm, 1 kHz pulses from a Ti:Sapphire laser were used as the driving and heating radiation, respectively (Fig. 1). The heating 200 ps pulses (HP) were focused using a 300-mm focal length cylindrical lens (CL) on the target (T) placed in the vacuum chamber to form a homogeneous extended plasma ($l = 5$ mm). MSM was installed between the cylindrical lens and the target to produce a MJP. We used three masks with different slit sizes: two with 0.2 and 0.5 mm slits separated by 0.2 and 0.5 mm from each other (MSM1 and MSM3) and one with a slit size of 0.8 mm separated by a 0.3 mm shield between the slits (MSM2, see the insets in Fig. 1). The plasma formation was accomplished 40 ns prior to the propagation of the 30 fs pulses (FPs) focused using the spherical lens (SL) along the MJP. The generated harmonics were propagated through the slit (S) in an XUV spectrometer.[8]

Silver microparticles (70 μm), boron nanoparticles (100 nm), bulk silver sulfide, and bulk silver were used as the targets. The powdered microparticles, nanoparticles, and mixtures of microparticles and nanoparticles were pressed to form tablets of 10-mm diameter. A part of the heating pulse was blocked by the MSM,

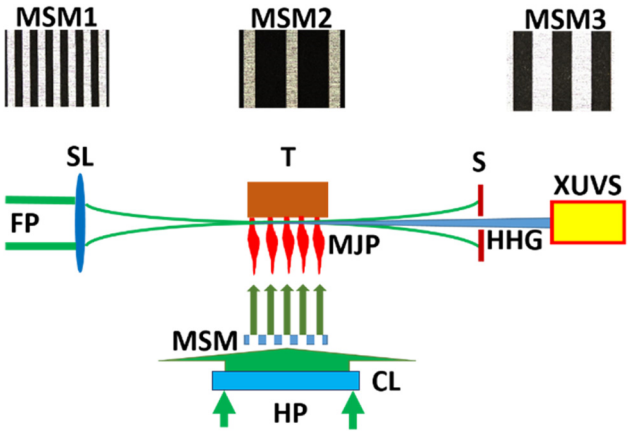

FIG. 1. QPM-HHG in MJP. The dark areas shown in the top panels correspond to the openings in the masks.

while the fluence of this radiation in the ablated area on the target surface (~1 J cm^{-2}) remained almost unchanged compared with the extended plasma.

III. RESULTS

Figure 2 shows the plateaulike and QPM-induced shapes of the odd harmonics generated in the plasmas produced on the (a) bulk Ag_2S, (b) bulk silver, and (c) mixture of boron nanoparticles and silver microparticles (at the weight ratio of 100:15) in the case of imperforated 5-mm long plasmas and different MJPs using the 800 nm, 30 fs driving pulses. The harmonics between the 7th (H7) and 47th (H47) orders are shown. One can see approximately the same plateaulike distribution of the harmonics generated in the extended 5-mm long plasmas (red-dashed curves in all three panels), in accordance with the three-step model of HHG.[9]

The envelopes of the generated spectra of harmonics drastically changed after we inserted different MSMs on the path of the heating picosecond radiation. The examples of three strongly modulated and enhanced spectra of the groups of odd harmonics compared to the case of homogeneous plasmas are shown as blue solid curves in Fig. 2. Particularly, the installation of MSM2 in front of the Ag_2S target significantly suppressed the lower-order harmonics, while the higher orders became enhanced in the range of H19–H31 [Fig. 2(a)]. An even stronger difference of these spectra is seen in the case of bulk silver plasma [Fig. 2(b)]. The lower-order harmonics from the MJP produced using MSM3 almost disappeared up to H25, while the higher-order harmonics centered at H33 prevailed over those generated in the imperforated plasma. The most prominent difference in the harmonics spectra from the imperforated and perforated plasmas was observed in the case of ablation of the mixture of boron nanoparticles and silver microparticles [B NPs + Ag MPs, weight ratio 100:15, Fig. 2(c)]. Almost no harmonics were generated above H19 in the extended plasma (red-dashed curve), while the modification of the homogeneous plasma shape using the MSM1 allowed the generation of the group of enhanced harmonics far from the above-mentioned cutoff (blue solid curve). Harmonics up to H47 are seen in this spectrum, while the strongest harmonics were centered at around H29–H33.

These three groups of QPM-induced spectra contain significantly enhanced high-order harmonics. The twofold decrease of the whole length of the MJP compared to the extended imperforated plasma (2.5 and 5 mm, respectively) did not play an important role in the yield of harmonics. This reveals the significant advantage of QPM HHG compared to ordinary HHG in extended plasmas.

The energy of the heating pulse producing MJPs on the surface of bulk silver plays an important role after one considers the variations of QPM conditions (Fig. 3). Previously, this dependence has demonstrated the influence of a larger concentration of plasmas and electrons on the formation of QPM conditions for different groups of harmonics. Particularly, the tuning of the maximum of spectral envelope (H_{qpm}) toward the lower-order harmonics with an increase of the flux of heating radiation has been reported in Ref. 2. An increase of electron concentration (N_e) in LPP at a stronger excitation of the target led to optimization of

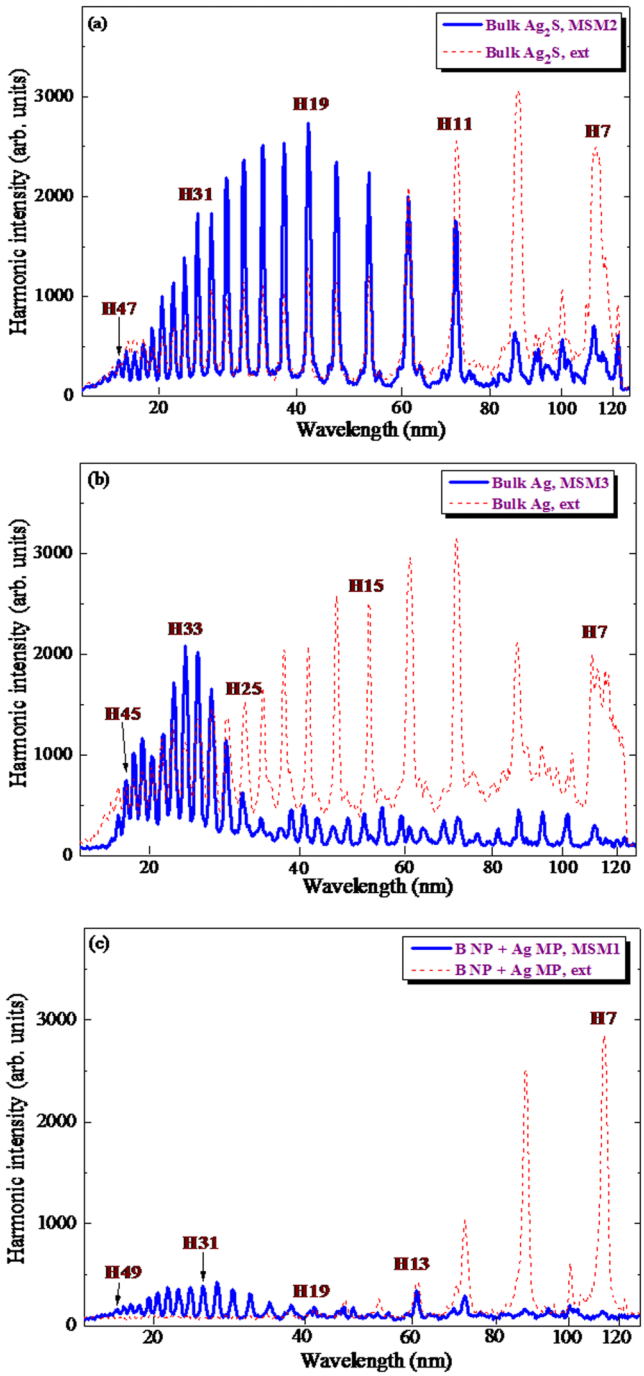

FIG. 2. Generation of high-order harmonics in different configurations of LPP. (a) Extended imperforated plasma (red-dashed curve) and MJP obtained using MSM2 (blue solid curve); bulk silver sulfide target. (b) Extended imperforated plasma (red-dashed curve) and MJP obtained using MSM3 (blue solid curve); bulk silver target. (c) Extended imperforated plasma (red-dashed curve) and MJP obtained using MSM1 (blue solid curve); pressed tablets containing boron nanoparticles and silver microparticles.

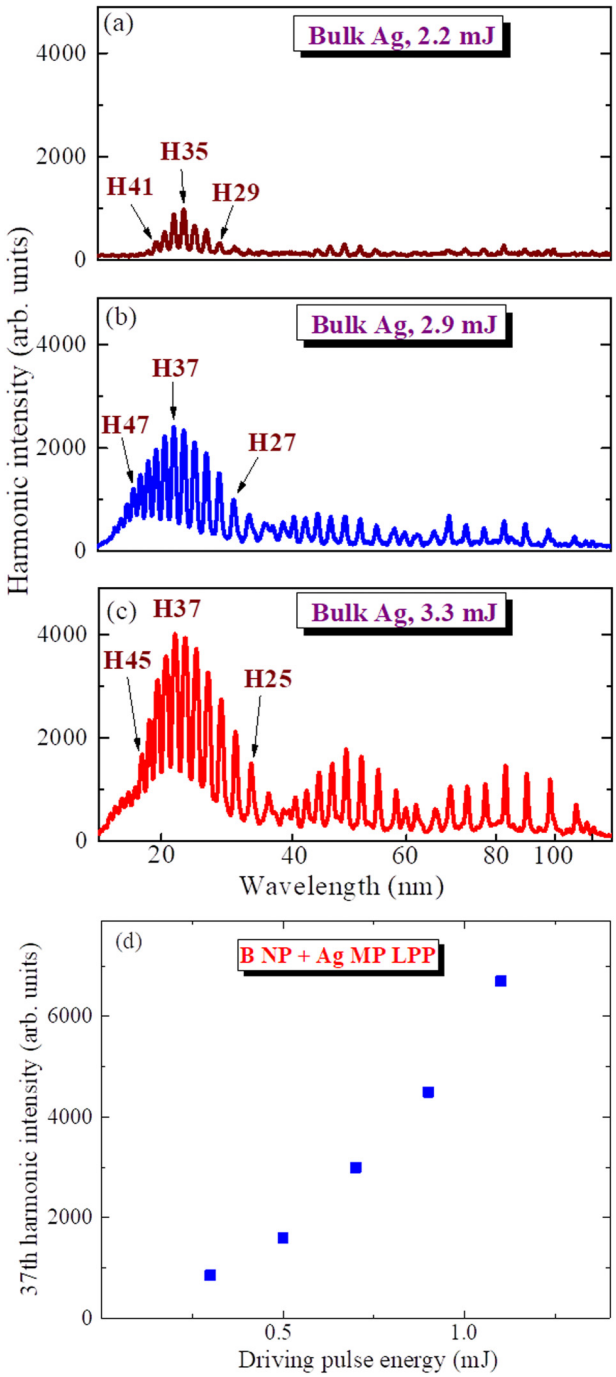

FIG. 3. (a)–(c) Harmonic distributions obtained during the propagation of femtosecond pulses through MJP produced on the surface of the bulk silver target using different energies of heating pulses. (a) 2.2 mJ, (b) 2.9 mJ, (c) 3.3 mJ. (d) Maximally enhanced harmonic (H37) yield as the function of the driving pulse energy in the case of HHG in the perforated B NP + Ag MP LPP. Maximally enhanced QPM harmonic (H37 or H39) was maintained at the conditions of variable energy of driving 30 fs pulses.

QPM for lower-order harmonics to keep the product $H_{qpm} \times N_e$ unchanged at the fixed spatial characteristics of plasma jets.[10]

Meanwhile, at conditions when the growth of the heating pulse's energy does not significantly change the concentration of electrons, the maximal order of enhanced harmonics remains almost the same. In the present studies, H_{qpm} corresponded to H35 or H37 in the case of Ag bulk plasma produced by pulses of different energy and perforated using MSM1 [Figs. 3(a)–3(c)]. The difference in these three spectra is attributed exclusively to (a) a larger amount of harmonic emitters and (b) the formation of better QPM conditions for a stronger excitation of the bulk target. The growth of plasma concentration led to an enhancement of conversion efficiency after the energy of the heating pulses was changed from 2.2 mJ [Fig. 3(a)] to 2.9 mJ [Fig. 3(b)] and to 3.3 mJ [Fig. 3(c)].

Notice the almost complete disappearance of the lower-order harmonics in these three spectra. The lines in the longer wavelength part of spectra correspond to the second and third orders of diffraction of the enhanced groups of harmonics. The presence of second- and third-order diffractions of enhanced harmonics is also seen in Fig. 2, though it is not as clear as in the case of Fig. 3, when the entire suppression of lower-order harmonics was achieved. This peculiarity allowing the disappearance of some harmonics and amendment of other harmonics is an important finding of the present study, which has never been reported. It means that we have determined the conditions when the macroscopic nonlinear optical process leading to the selection of the group of phase-matched harmonics drastically overpasses the microscopic process of HHG, leading to an almost homogeneous distribution of harmonics.

We also analyzed QPM conditions at different energies of driving femtosecond pulses [0.3–1.1 mJ, Fig. 3(d)]. The envelope of enhanced harmonics was centered at around H37–H39 when we used the 2.6 mJ, 200 ps heating pulses and MSM1 with 0.2 mm slits. H_{qpm} was almost the same in the case of five different energies of driving pulses since the concentration of the free carriers responsible for QPM for some specific harmonic order remained unchanged during these experiments due to the same energy of the heating picosecond pulses. With these experiments, we defined that the free carriers appearing during the propagation of the driving femtosecond pulses through the plasma did not strongly affect the QPM conditions. The only difference in these five cases of the growing femtosecond pulse energies was the gradual enhancement of the intensity of H_{qpm} alongside a few surrounding harmonics. We also observed the broadening of the envelope of harmonic distribution centered at around H_{qpm} with the growth of the energy of the driving pulse.

The plasma produced from the tablets containing only boron nanoparticles did not show the creation of conditions when the higher-order harmonics become enhanced. The formation of perforated plasmas on the Ag MP-containing tablets (i.e., without B NPs) allowed the generation of enhanced harmonics compared with the imperforated plasma in the spectral range where no harmonics from the extended plasma were seen (Fig. 4).

The comparison of harmonic yields was carried out at similar conditions of experiments and data collection. We compared two spectra of harmonics generated with and without the insertion of the MSM on the path of the heating beam. Particularly, in Fig. 2, we showed how the harmonic yield modifies in different spectral ranges during insertion of three MSMs distinguished by different sizes of slits, independently of the material used for ablation. Thus, the same intensity of harmonics scales in this figure for the extended imperforated and perforated plasmas. The same can be said about the comparative curves presented in Fig. 4.

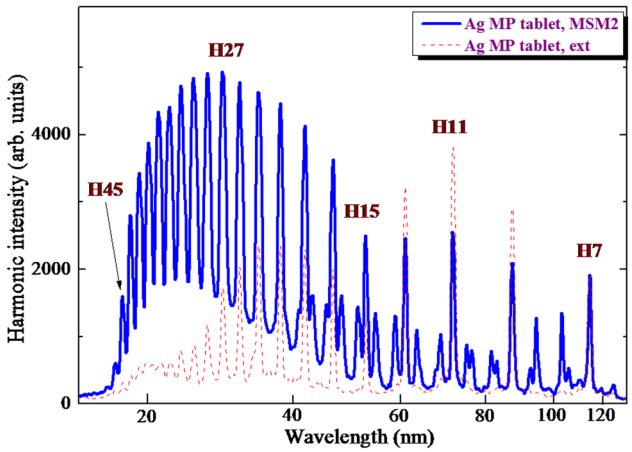

FIG. 4. Harmonic intensity distributions obtained in the extended imperforated plasma (red-dashed curve) and MJP produced using MSM2 (blue solid curve) on the surface of Ag MP-containing tablets.

We also carried out QPM-HHG at the conditions of the two-color pump (TCP) of plasma[11–15] using 800 nm (97%) and 400 nm (3%) radiation. Figure 5 demonstrates the raw images of harmonic spectra obtained using single-color pump (SCP) and TCP of extended Ag plasma. We also show the harmonic spectrum

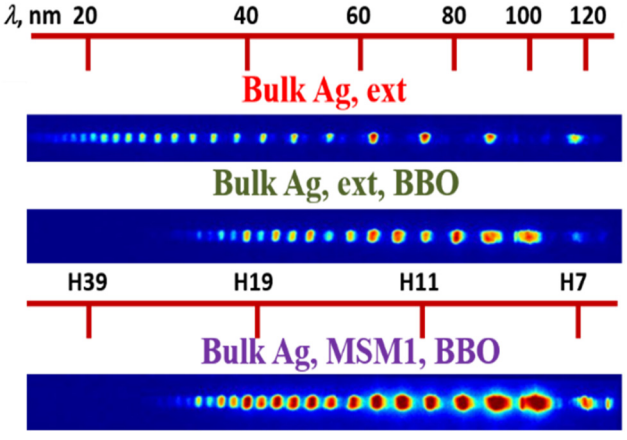

FIG. 5. Harmonic spectra obtained using SCP (upper panel) and TCP (middle panel) of the extended Ag plasma. The bottom panel shows the harmonic spectrum generated in the perforated plasma produced using MSM1 in the case of TCP.

generated in the perforated Ag plasma produced using MSM1 in the case of TCP. The conversion efficiency in the case of TCP (Fig. 5, middle panel) was higher than that in the case of the single-color pump (SCP, Fig. 5, upper panel) of the extended plasma. The decrease in the generation of higher order harmonics did not allow the observation of their enhancement in the case of MJP relative to the case of SCP of the perforated plasma (Fig. 5, bottom panel).

IV. DISCUSSION

A previous analysis of the intensity of harmonics as a function of the number of plasma jets provided a proof of the decisive role of QPM in the variations in the harmonics spectrum.[2,16] A recent analysis of the phase shift of harmonics along a plasma using the analytical solution of nonlinear wave equation allowed the determination of two regimes of phase matching at the conditions of SCP—compensation of dispersion-induced phase mismatch by the Gouy phase in extended plasmas and QPM-HHG using the phase change due to free electrons in the space between plasma jets.[17]

Our studies showed that the influence of the second harmonic was sufficient to strongly modify the whole harmonic spectrum compared to SCP in the case of extended imperforated plasmas. Meanwhile, the formation of MJP and application of TCP did not lead to a strong QPM-induced enhancement of some groups of harmonics and depression of the lower parts of harmonic spectra. The coherence length of the qth harmonic is determined as

$$L_{coh} \approx 4\pi^2 m_e \varepsilon_0 c^2 / q N_e e^2 \lambda, \quad (1)$$

where λ is the wavelength of the driving radiation; N_e, m_e, and e are the density, the mass, and the charge of an electron, respectively; c is the velocity of light, and ε_0 is the permittivity of vacuum.[18] One can deduce from this relation the dependence between a maximally enhanced harmonic and the laser wavelength ($H_{\mathrm{qpm}} \propto \lambda^{-1}$). Correspondingly, the use of twice shorter wavelength leads to the twofold increase of the order of the maximally QPM-enhanced harmonic. Thus, the observation of QPM at these conditions is possible only when the plasma medium allows the generation of a twice longer cutoff in the silver plasma (i.e., up to ~ 100th order). Since this medium cannot provide those harmonics, QPM also cannot be observed.

In the case of homogeneous irradiation of targets, the Ag, B NPs + Ag MPs, and Ag_2S plasmas allowed the generation of the plateaulike distribution of harmonic intensities. Therefore, MJP setups led to a clear observation of QPM at SCP. The maximally achieved enhancement factor for H33 in the case of MJP compared to the extended (5-mm-long) plasma was measured to be 22× in the case of B NPs + Ag MP plasmas.

We did not make the absolute measurements of harmonic conversion efficiency at QPM conditions in laser produced plasmas. Meanwhile, the estimates of conversion efficiency were carried out using the comparison with the earlier reported measurements of this parameter in Ag plasmas at similar experimental conditions. By knowing the conversion efficiency from previous measurements of harmonic generation in the plasmas produced on the surface of bulk Ag (8×10^{-6}, Ref. 19), we determined the conversion efficiency for maximal QPM-enhanced harmonic (3×10^{-5}). The conversion efficiencies in extended Ag, B NPs + Ag MPs, and Ag_2S plasmas in the present experiments were estimated to be 4×10^{-6}, 1×10^{-6}, and 3×10^{-6}, respectively. The corresponding conversion efficiencies for maximal QPM-enhanced harmonics were calculated to be 3×10^{-5}, 2×10^{-5}, and 3×10^{-5} for the MJPs produced on bulk Ag, B NPs + Ag MPs, and bulk Ag_2S targets, respectively.

The pioneering studies of QPM in plasmas[2] have revealed the potential materials for efficient enhancement of the group of high-order harmonics in different ranges of extreme ultraviolet. Apart from silver, materials such as manganese and indium allowed achieving QPM in laser produced plasmas. All of these materials have demonstrated the generation of high-order harmonics. Even the weak higher-order harmonics generation is a sufficient requirement for observation of their enhancement at matching the group velocities of the driving and converted waves. In the present studies, we have chosen other materials, which showed potential for the generation of a strong coherent emission through HHG. The advantages in the application of multiatomic species (clusters and nanoparticles) for plasma HHG demonstrated in earlier studies allowed us to expect their efficient application during implementation of the QPM concept.

The choice of the multislit masks was also based on previous applications of different plasma jets. Earlier, perforated plasma generated using a mask containing 0.3-mm slits allowed achieving the enhancement of the group of harmonics centered at around H30. We have chosen MSM containing 0.2-mm slits for demonstrating the shift of a maximally enhanced harmonic toward the shorter-wavelength range of XUV assuming the equality of the plasma length of each of ten generated jets (0.2 mm) and the coherence length of the higher order of harmonic (~H35) at the "optimal" fluence of the heating beam allowing the appearance of a sufficient amount of free electrons. Correspondingly, the application of larger-sized slits, like 0.8 mm, led to an enhancement of the lower orders of harmonics. The implementation of five 0.5-mm slits caused the intermediate harmonics enhancement.

The yet studied issue was the application of the smaller distance between the slits compared with the slit sizes, i.e., the mask having a 0.3-mm distance between 0.8-mm slits. We wanted to analyze this issue, since some of the assumptions involved in the consideration of the role of free electrons in the no-plasma area predicted the independence of this parameter on the harmonic enhancement. Our studies have revealed that the distance between slits does not influence the QPM conditions, provided the whole plasma area is contained within two Rayleigh lengths of the driving radiation.

Our studies showed that TCP cuts out the high harmonics between 40 nm and less than 20 nm compared to SCP (Fig. 5). Some explanation of this effect can be related to the use of the twice shorter wavelength source as one of the two pumps in the TCP scheme. The relation of the three-step model provides the dependence of the cutoff energy, the ionization potential (E), and the ponderomotive potential (U_p) when the former parameter scales as $E + 3.2U_p$. Because of the λ^2 dependence of the ponderomotive energy ($U_p \propto I_0 \lambda^2$), one can assume a decrease of the harmonic cutoff with the decrease of the driver wavelength. In the meantime, the integrated harmonic yield of the isolated atom scales as λ^{-5}. With a

decrease of the driving wavelength, the recombination of the electron wave packet with the parent ion becomes increasingly efficient, thus increasing the HHG yield. It has been a common feature for both gas and plasma HHGs to achieve a stronger yield of harmonics from a 400 nm driving wave with regard to an 800 nm radiation, while the cutoff energy decreased in the former case.

In our case, we used a strong first field (800 nm) and a weak second field (400 nm) to pump the plasma plume. We showed that even a 30:1 ratio between these two fields dramatically changes the spectrum of harmonics, which point out the decisive influence of a weak second field on the whole process of HHG. A similar influence could be expected after one considers the variation of cutoff for TCP vs SCP schemes. The decrease of cutoff did not follow the quadratic dependence on the wavelength, though we observed the almost twofold decrease of the maximally generated harmonic order and the stronger odd harmonics in the case of TCP.

V. CONCLUSIONS

In conclusion, we have reported the high-order harmonics generation at quasi-phase-matched conditions in silver microparticles and silver sulfide plasmas of different configurations. We have demonstrated QPM of the high-order harmonics generated in the plasmas containing silver microparticles and atoms, boron nanoparticles, and silver sulfide molecules. The influence of the flux of the heating beam, as well as variations of the geometry of multijet plasmas, on the maximally enhanced harmonic has been demonstrated. The groups of harmonics in the range of 30th to 50th orders at QPM conditions prevailed over the lower orders of harmonics. In most cases, the lower-order harmonics fully disappeared from the generated spectra at QPM conditions. The enhancement factors of QPM harmonics up to 22× were demonstrated in the case of mixed boron nanoparticle and silver microparticle plasmas for the harmonics in the energy range of 47–67 eV. The conversion efficiencies for QPM-enhanced harmonics were estimated to be 3×10^{-5}, 2×10^{-5}, and 3×10^{-5} for the MJPs produced on the bulk Ag, B NPs + Ag MPs, and Ag_2S targets, respectively.

ACKNOWLEDGMENTS

Financial support from the National Key Research and Development Program of China (Nos. 2017YFB1104700 and 2018YFB1107202), the National Natural Science Foundation of China (NNSFC) (Nos. 91750205 and 61774155), the Scientific Research Project of the Chinese Academy of Sciences (CAS) (No. QYZDB-SSW-SYS038), the Russian Foundation for Basic Research (RFBR) (No. 17-52-12034 ННИО_а), and the Key Program of the International Partnership Program of CAS (No. 181722KYSB20160015) is appreciated. R.A.G. thanks financial support from the Chinese Academy of Sciences President's International Fellowship Initiative (Grant No. 2018VSA0001).

REFERENCES

[1]P. B. Corkum and F. Krausz, Nat. Phys. **3**, 381 (2007).
[2]R. A. Ganeev, M. Suzuki, and H. Kuroda, Phys. Rev. A **89**, 033821 (2014).
[3]M. Wöstmann, L. Splitthoff, and H. Zacharias, Opt. Express **26**, 14524 (2018).
[4]J. Seres, V. S. Yakovlev, E. Seres, C. H. Streli, P. Wobrauschek, C. H. Spielmann, and F. Krausz, Nat. Phys. **3**, 878 (2007).
[5]A. Pirri, C. Corsi, and M. Bellini, Phys. Rev. A **78**, 011801 (2008).
[6]V. Tosa, V. S. Yakovlev, and F. Krausz, New J. Phys. **10**, 025016 (2008).
[7]T. Fok, Ł Węgrzyński, M. Kozlova, J. Nejdl, P. W. Wachulak, R. Jarocki, A. Bartnik, and H. Fiedorovicz, Photonics Lett. Pol. **6**, 14 (2014).
[8]R. A. Ganeev, G. S. Boltaev, V. V. Kim, K. Zhang, A. I. Zvyagin, M. S. Smirnov, O. V. Ovchinnikov, P. V. Redkin, M. Wöstmann, H. Zacharias, and C. Guo, Opt. Express **26**, 35013 (2018).
[9]P. B. Corkum, Phys. Rev. Lett. **71**, 1994 (1993).
[10]R. A. Ganeev, A. Husakou, M. Suzuki, and H. Kuroda, Opt. Express **24**, 3414 (2016).
[11]C. M. Kim and C. H. Nam, J. Phys. B **39**, 3199 (2006).
[12]T. Pfeifer, L. Gallmann, M. J. Abel, D. M. Neumark, and S. R. Leone, Opt. Lett. **31**, 975 (2006).
[13]D. Charalambidis, P. Tzallas, E. P. Benis, E. Skantzakis, G. Maravelias, L. A. A. Nikolopoulos, A. P. Conde, and G. D. Tsakiris, New J. Phys. **10**, 025018 (2008).
[14]R. A. Ganeev, H. Singhal, P. A. Naik, I. A. Kulagin, P. V. Redkin, J. A. Chakera, M. Tayyab, R. A. Khan, and P. D. Gupta, Phys. Rev. A **80**, 033845 (2009).
[15]R. A. Ganeev, J. Opt. Soc. Am. B **33**, E93 (2016).
[16]R. A. Ganeev, V. Tosa, K. Kovács, M. Suzuki, S. Yoneya, and H. Kuroda, Phys. Rev. A **91**, 043823 (2015).
[17]P. V. Redkin, R. A. Ganeev, and C. Guo, J. Phys. B **52**(7), 075601 (2019).
[18]L. Zheng, X. Chen, S. Tang, and R. Li, Opt. Express **15**, 17985 (2007).
[19]R. A. Ganeev, M. Baba, M. Suzuki, and H. Kuroda, Phys. Lett. A **339**, 103 (2005).